RF DESIGN PROGRESS OF THE 197 MHz CRAB CAVITY FOR EIC*

B. Xiao[†,1], J. C. Brutus[1], A. Blednykh[1], Z. Conway[2], J. Cox[2], J. R. Delayen[2,3], S. U. De Silva[3],
R. Fernandes[2], J. Guo[2], D. Holmes[1], N. Huque[2], G. Li[1], Z. Li[4], J. B. Mandel[2],
S. Verdú-Andrés[1], G. Wang[1], Q. Wu[1], W. Xu[1]
[1]Brookhaven National Laboratory, Upton, New York, USA
[2]Thomas Jefferson National Accelerator Facility, Newport News, VA, USA
[3]Center for Accelerator Science, Old Dominion University, Norfolk, VA, USA
[4]SLAC National Accelerator Laboratory, Menlo Park, CA, USA

Abstract

The interaction region (IR) crab cavity system is a special RF system designed to recover head-on collision since there will be luminosity loss caused by the 25 mrad crossing angle at the interaction point (IP) of the Electron-Ion collider (EIC). The configuration includes six crab cavities in the Hadron (proton or ion) Storage Ring (HSR) installed on each side of the IP, four operating at 197 MHz and two at 394 MHz, along with one (or two) 394 MHz crab cavity on each side of the IP in the Electron Storage Ring (ESR). This paper presents the recent progress in the RF design of the 197 MHz crab cavity, addressing the geometrical constraints, required crabbing voltages, multipole components, and the Higher Order Mode (HOM) power and impedance thresholds.

INTRODUCTION

The EIC crab cavities are designed to provide local crabbing scheme in the horizontal plane for two possible interaction points (IPs), with 197 MHz and 394 MHz for hadron storage ring (HSR) and 394 MHz for electron storage ring (ESR). Challenges include large cavity size, longitudinal and transverse space constraints in both IPs, tight impedance budget, and beyond the state-of-art low level RF (LLRF) control specs [1, 2]. In this paper, we focus on the design of the 197 MHz crab cavity RF components, including the Fundamental Power Coupler (FPC), Higher Order Mode (HOM) dampers, pickup couplers and beamline bellows.

197 MHz HSR CRAB CAVITY

Both Double Quarter Wave (DQW) and RF-dipole (RFD) designs were adopted in High Luminosity Large Hadron Collider (HL-LHC) at 400 MHz. For the 197 MHz crab cavity for EIC HSR, both DQW and RFD were considered, and the RFD was chosen majorly due to the stiffeners and components added to the cavity system are more complex in the DQW [3]. RFD design is simpler and closer to the HL-LHC version while comparing with DQW. Two designs were proposed for the RFD HOM damper, one with waveguide absorbers, and the other with coaxial absorbers. Coaxial design was chosen over the waveguide design due to its simplicity on design and mechanical integration [3-5]. Recent progress of the cavity design and fabrication has been covered in [6], in which the cavity optimization includes changing the capacitive poles from flat surface for the prototype cavity [7] to curved surface for the production cavity [8] to meet the requirement on multipole components [9, 10]. Due to this change, the number of coaxial dampers for each cavity has increased from 3 to 4 [8]. In this paper, the RF design progress of the 197 MHz crab cavity RF components for EIC will be covered. Figure 1 shows the RF components of this cavity, including one FPC, two HOM dampers on VHOM waveguide, two HOM dampers on HHOM waveguide, two pickup couplers on HHOM waveguide per cavity, as well as two warm-cold bellows and one cold-cold bellows per cryomodule, with two cavities per cryomodule.

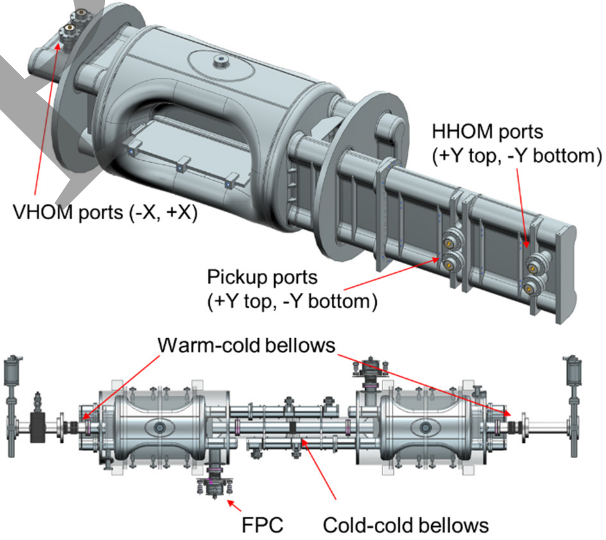

Figure 1: EIC HSR 197 MHz crab cavity with RF components.

FUNDAMENTAL POWER COUPLER

With a beam offset of $\Delta x = 0.6$ mm and microphonic detuning of $\delta f = 50$ Hz for a beam current of 1.0 A and cavity $[R/Q]_t = 1034\ \Omega$, FPC's external quality factor should be $Q_{ext} = 1.75\times10^6$ for optimal power requirement. With this the maximum power required at the cavity is 50 kW, it is

---

* Work supported by Brookhaven Science Associates, LLC under Contract No. DE-SC0012704 with the U.S. Department of Energy, and by DOE Contract No. DE-AC02-76SF00515. This work used computer resources at the National Energy Research Scientific Computing Center.

[†] binping@bnl.gov

designed to deliver 60 kW power to the cavity with 75 kW amplifier.

The 400 kW FPC window designed for the EIC ESR 591 MHz SRF cavity is used [11]. With FPC at lower frequency, it performs better with reduced reflection (S_{11} lowered from -40 dB at 591 MHz to -50 dB at 197 MHz). Instead of the waveguide to coax transition used in 591 MHz SRF cavity, a quarter wave (QW) stub will be used in 197 MHz crab cavity to provide water cooling to the inner conductor due to its simpler and compact structure, as well as lower cost while comparing with waveguide to coax design.

The inner conductor diameter is designed to have an impedance of 75 Ω in vacuum tapered up to 50 Ω near the RF window, in order to suppress multipacting resonances without DC bias [8]. The inner conductor is shorter while comparing with the inner conductor length of the ESR 591 MHz SRF cavity. Thermal contraction from room temperature to cryogenic temperature has been considered so that the insertion of the inner conductor can provide the right FPC Q_{ext} during operation.

A 5g load in all directions during transportation has been considered in simulation. Results showed that by adopting the air-side support that was originally designed for 591 MHz SRF cavity, such a load results in a peak stress of 1.7 ksi in the copper cylinder adjacent to the vacuum-side window ID, which is well below the 2.33 ksi yield stress of Cu after brazing. The FPC window can be handled and shipped safely.

To better understand the power dissipation on the Cu or Cu coated FPC inner and outer conductor, precise simulation on the travelling wave and standing wave of the cavity with up to 60 kW RF power, with and without beam loading, is needed. According to Panofsky-Wenzel theorem, the crabbing voltage V_t can be calculated from the gradient of the longitudinal voltage $V_{//}(y)$ with y the offset: $V_t = -i\frac{1}{\kappa}\frac{V_{//}(y)}{y}$, with the assumption that there is no longitudinal voltage with 0 offset: $V_{//}(0) = 0$. There is a 90° (or -90° depending on the sign of offset y) phase difference between crabbing voltage at its maximum and longitudinal voltage, together with the 90° (or -90° depending on how the beam get crabbed) phase advance between the crabbing mode and the crabbing voltage at its maximum, the phase difference between the crabbing mode and the longitudinal voltage would be either 0° or 180°, meaning that the beam loading could be either consuming or generating power.

This conclusion was applied to the thermal simulation for FPC inner and outer conductor [12] together with the QW stub. Results showed a maximum loss of 197 W and 5.9 W on inner and outer conductors, respectively. The outer conductor will have a warm-to-cold transition like the ESR 591 MHz cavity design which can handle this maximum RF power level. The inner conductor will have water cooling from QW stub that can handle the maximum RF power generated on it. For the QW stub, the temperature on the inner conductor will increase to a maximum of 60°C, on the outer conductor will be 34°C maximum, and on the Polytetrafluoroethylene (PTFE) that support the inner conductor and isolate it from the outer conductor will be 118°C. Rexolite® is a good alternative to PTFE if needed.

HOM DAMPER AND PICKUP COUPLER

Four HOM dampers and two pickup couplers are used in this cavity. They all use the same RF window design that is modified from CERN design for LHC crab cavities (see Figure 2.). Identical inner conductors with flat plates are used in all HOM dampers to ensure identical vacuum components. The two pickup couplers use simple straight probes and are identical. For HOM dampers, LHC cables will be used together with commercially available Bird® 8726 water-cooled (2 gpm flow) coax loads. RF simulations have been performed using realistic material properties of different materials (Nb, Cu coating, ceramic window) and VSWR of the coax loads, together with different bunch patterns. Results are shown in Table 1, with first part RF power dissipation on different components and second part RF power extraction from six different ports shown in Figure 1. Both fundamental and HOM power are considered, with first column showing the effect from fundamental mode at 11.5 MV deflecting voltage (the extreme case), second column showing the effect from all HOMs up to 2 GHz for 1160 bunches with 1 Amp and 6 cm bunch length (HOM Case 1), third column showing the same effect for a different bunch pattern with 290 bunches with 0.74 Amp and 6 cm bunch length (HOM Case 2), and fourth column showing the first row plus the larger number from the second and third rows, the worst case. For the HOM power, a maximum of 0.6 mm beam offset with ±0.2% HOM frequency uncertainty (assuming within this range it aligns to the maximum of beam spectrum) is considered.

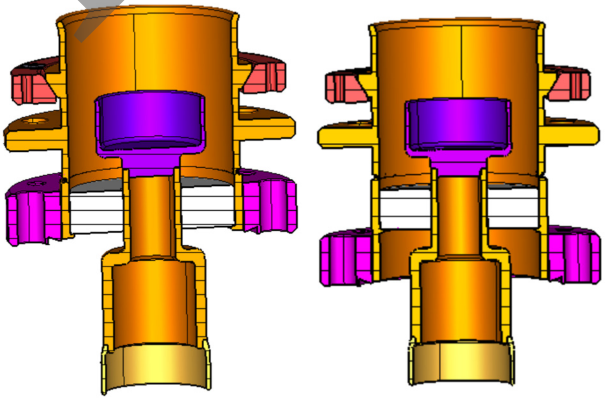

Figure 2: RF window for HOM dampers and pickup couplers. Left: JLab version for LHC crab cavities; right: Modified for EIC crab cavities.

Thermal simulations are done based on the RF power shown above. Boundary conditions are set with cooling from 2 K helium vessel, 4 K strap near the HOM ports, 60 K thermal intercept on the HOM cable outer conductor at 60% of the length from the warm side, and room temperature at the end of the HOM cable. With 3.8 kW power on a single HOM load, the inner conductor maximum temperature will be 350 K. The actual power on each load will be less than that, no more than 1.9 kW as shown in Table 1. Temperature on Nb waveguide stub will be below 4.5 K, and on indium seal at waveguide joint (with 3.4 K critical temperature) remains below 2.8 K. Per HOM damper, there will be 1.6 W power dissipation on 60 K thermal intercept, 1.6 W power dissipation on 4 K strap, with 0.6 W from outer conductor and 1 W from inner conductor. Further optimization will be done to identify if the 60 K thermal intercept can be removed.

Table 1: Fundamental and HOM Power Dissipation and Extraction on HOM Dampers and Pickup Couplers

	Fundamental	**HOM Case 1**	**HOM Case 2**	**Worst case**
Power dissipation [W]				
HHOM WG Stub (Nb, 4 K)	2.9e-3	4.7e-6	2.1e-5	3.0e-3
VHOM WG Stub (Nb, 4 K)	1.0e-5	1.4e-5	1.3e-5	3.0e-5
VHOM antenna (-X)	0.10	0.52	0.34	0.62
VHOM antenna (+X)	0.17	0.65	0.49	0.82
HHOM antenna (-Y)	0.052	0.069	0.35	0.40
HHOM antenna (+Y)	0.040	0.089	0.22	0.26
Pickup antenna (-Y)	0.11	0.0012	0.0030	0.11
Pickup antenna (+Y)	0.11	0.0011	0.0030	0.11
Power extraction [W]				
VHOM port (-X)	32.2	1420.6	1068.4	1455.0
VHOM port (+X)	79.1	1807.1	1330.3	1887.0
HHOM port (-Y)	31.1	154.5	850.3	882.0
HHOM port (+Y)	56.9	185.1	531.1	591.0
Pickup port (-Y)	5.0	0.61	2.6	7.6
Pickup port (+Y)	5.0	0.62	1.7	6.7

RF power emitted from beampipes are calculated using wake field simulation with HOM ports and beampipe ports. Beam from both directions (VHOM side to HHOM side and vice versa since in the cryomodule two cavities are back-to-back) are considered. Results reveal that RF power emitted from beampipe ports will be less than 1 W per port.

Tolerance studies were reported previously to suggest the fabrication and assembly tolerances [13, 14], and there is no multipacting on the HOM waveguides and coaxial lines, nor on the FPC waveguide and coaxial line.

HOM power leak through the pickup couplers is not large (2.6 W maximum) and can be filtered using a low power low pass filter. Q_{ext} of pickup couplers are set at $2.70 \sim 3.24 \times 10^{10}$ to provide 5 W needed by LLRF.

BELLOWS

Bellows for this cavity were previously reported in [15]. Longitudinal short-range wake is small compared with other components in HSR, while the transverse short-range wake needs special attention as it got amplified by the horizontal beta function β_x at crab location (1300 m, ~50 times larger than beam screen location). A recent study showed that an unshielded low impedance design proposed by Wu [16] with 6 convolutions in a bellows, 3 on each side that are separated by a straight section, can provide the longitudinal (2.2 mm) and transverse (0.7 mm) movements needed for this cryomodule for both warm-cold and cold-cold bellows. Short-range wake simulation showed a 0.041 V/pC/m transverse loss factor k_x per bellows, with a total 12 warm-cold and cold-cold bellows, $12k_x\beta_x$ = 640 V/pC, ~70% of the contribution from the beam screen. These bellows are acceptable for beam stabilities and can be used both as warm-cold and cold-cold bellows.

SUMMARY

RF components for EIC 197 MHz crab cavity were studied. Power dissipation on FPC including inner and outer conductors inside and outside the vacuum together with the ceramic window and QW stub was calculated, thermal simulation showed that a maximum of 60°C temperature on metal surface. HOM power leak through the pickup couplers is not large (2.6 W maximum) and can be filtered. RF power dissipation on each component, as well as RF power extraction through each HOM port, are calculated. Thermal simulation based on it showed reasonable temperature distribution on HOM waveguides and coax lines. Unshielded low impedance bellows can be used both as warm-cold and as cold-cold bellows in this cryomodule.

REFERENCES

[1] H. Huang *et al.*, "Emittance Growth Due to RF Phase Noise in Crab Cavities", in *Proc. NAPAC'22*, Albuquerque, NM, USA, Aug. 2022, pp. 708-710. doi:10.18429/JACoW-NAPAC2022-WEPA36

[2] T. Mastoridis, P. Fuller, P. Mahvi, and Y. Matsumura, "EIC Transverse Emittance Growth Due to Crab Cavity RF Noise: Estimates and Mitigation", in *Proc. NAPAC'22*, Albuquerque, NM, USA, Aug. 2022, pp. 6-8. doi:10.18429/JACoW-NAPAC2022-MOYD3

[3] B. Xiao *et al.*, "HOM Damper Design for BNL EIC 197 MHz Crab Cavity", in *Proc. SRF'21*, East Lansing, MI, USA, Jun.-Jul. 2021, pp. 624-626. doi:10.18429/JACoW-SRF2021-WEPCAV014

[4] B. Xiao *et al.*, "HOM power in the EIC crab cavity system", in *Proc. IPAC'24*, Nashville, TN, USA, May 2024, pp. 2720-2722. doi:10.18429/JACoW-IPAC2024-WEPS12

[5] S. De Silva, J. Delayen, J. Guo, Z. Li, R. A. Rimmer, and B. Xiao, "197 MHz Waveguide Loaded Crabbing Cavity Design for the Electron-Ion Collider", in *Proc. NAPAC'22*,

Albuquerque, NM, USA, Aug. 2022, pp. 679-682. doi:10.18429/JACoW-NAPAC2022-WEPA26

[6] S. De Silva *et al.*, “EIC crab cavity RF systems”, presented at SRF'25, Tokyo, Japan, Sep. 2025, paper MOA03, to be published.

[7] N. Huque *et al.*, “Development of a Prototype 197 MHz Crab Cavity for the Electron-Ion Collider at JLab”, in *Proc. SRF'23*, Grand Rapids, MI, USA, Jun. 2023, pp. 685-690. doi:10.18429/JACoW-SRF2023-WEPWB051

[8] Z. Li *et al.*, “EIC 197 MHz Crab Cavity RF Optimization”, in *Proc. SRF'23*, Grand Rapids, MI, USA, Jun. 2023, pp. 584-588. doi:10.18429/JACoW-SRF2023-TUPTB068

[9] Q. Wu, Y. Luo, B. Xiao, S. De Silva, and Z. Li, “Higher Order Multipole Analysis of Beam Crabbing Mode at 197 MHz for Electron-Ion Collider”, Rep. BNL-225439-2024-TECH, EIC-ADD-TN-089, USA, Mar. 2024. https://technotes.bnl.gov/PDF?publicationId=225439

[10] Q. Wu *et al.*, “EIC Crab Cavity Multipole Analysis and Their Effects on Dynamic Aperture”, in *Proc. IPAC'22*, Bangkok, Thailand, Jun. 2022, pp. 66-69. doi:10.18429/JACoW-IPAC2022-MOPOST009

[11] W. Xu *et al.*, “Progress on high power FPC development for EIC”, in *Proc. IPAC'24*, Nashville, TN, USA, May 2024, pp. 2727-2729. doi:10.18429/JACoW-IPAC2024-WEPS14

[12] S. De Silva *et al.*, “Thermal analysis for the fundamental power coupler of the 197 MHz crab cavity for EIC”, in *Proc. IPAC'25*, Taipei, Taiwan, Jun. 2025, pp. 1745-1748. doi:10.18429/JACoW-IPAC2025-WEPB013

[13] S. De Silva *et al.*, “Sensitivity analysis of the 197 MHz prototype crab cavity for EIC”, in *Proc. IPAC'25*, Taipei, Taiwan, Jun. 2025, pp. 1749-1752. doi:10.18429/JACoW-IPAC2025-WEPB014

[14] Z. Li, B. Xiao, S. U. D. Silva, Q. Wu, J. R. Delayen, and R. Rimmer, “EIC 197 MHz crab cavity HOM damping and tolerance analysis”, in *Proc. IPAC'25*, Taipei, Taiwan, Jun. 2025, pp. 821-824. doi:10.18429/JACoW-IPAC2025-MOPS137

[15] G. Li *et al.*, “Trapped mode and wakefield evaluation of bellows for 197 MHz superconducting crab cavities”, presented at SRF'25, Tokyo, Japan, Sep. 2025, paper MOP83, to be published.

[16] G. Wu *et al.*, “Low Impedance Bellows for High-current Beam Operations”, in *Proc. IPAC'12*, New Orleans, LA, USA, May 2012, paper WEPPC042, pp. 2303-2305.